Parameter sensitivities in the relativistic distorted-wave Born approximation model for the (p, π^+) reaction

E. D. Cooper

Nuclear Theory Center, Indiana University, Bloomington, Indiana 47405

H. S. Sherif

Nuclear Research Centre, University of Alberta, Edmonton, Alberta, Canada T6G 2N5
(Received 3 October 1983)

The sensitivities to input parameters of the (p, π^+) observables calculated using a relativistic one-nucleon distorted-wave Born approximation model are discussed. We investigate the effects of variations in bound state geometry and of ambiguities in the pion optical potential, as well as finite range effects in the production vertex.

A Dirac single nucleon approach to the (p, π^+) reactions[1,2] has recently been studied in detail by the present authors.[3,4] The basic ingredient of the model is the use of the Dirac equation to describe the nucleon motion with appropriately chosen vector and scalar nuclear potentials. The pion is described by a distorted wave generated from a pion optical potential using the Klein-Gordon equation. Both pseudovector and pseudoscalar forms of the πNN production vertex have been used and we have found strong evidence in favor of the former. These vertex functions were treated in a zero-range (ZR) approximation.

It is necessary in such models to make an assessment of the sensitivity of the final results to the various types of input parameters that enter these calculations. In this paper we make an attempt to investigate some of these sensitivities. We specifically discuss sensitivities to the bound state potentials, to the pion distortions, and to the range of the πNN vertex form factor. For illustrative purposes, we specialize throughout to the case of $^{40}Ca(p,\pi^+)^{41}Ca_{g.s.}$ with incident protons of energy 160 MeV, although the conclusions apply more generally.

In the relativistic DWBA approach to (p, π^+) reactions, the transition t-matrix element in the zero range approximation is given by[1-4]

$$T = i\sqrt{2} \int d^3r\, \bar{\psi}_n(\vec{r})\Gamma\psi_p^{(+)}(\vec{r})\phi_\pi^{*(-)}(\vec{r}) ,\qquad (1)$$

where ψ_n is a Dirac spinor describing the final state bound neutron and Γ is the pion production vertex. The spinor ψ_p represents the incident proton and ϕ_π is the pion distorted wave.

The potentials used to generate the bound state neutron wave function ψ_n are a combination of vector and scalar interactions. Their radial forms are taken to be Woods-Saxon functions. The geometry (radial and diffuseness) parameters for the vector and scalar potentials are taken to be the same, and are often based on geometries derived from fitting the incident proton elastic scattering data. The range of values found for the radial parameter is (1.0–1.06) fm, the range of values for the diffuseness (0.6–0.7) fm. In Fig. 1 we show the variations which take place in the predicted cross sections upon varying these

parameters. The variations in these parameters are made larger than the numbers just quoted so as to illustrate the trends. It can be seen that changing the radial parameter leads to a shift in the position of the minimum as well as a change of normalization, whereas changing the diffuseness parameter mainly alters the overall magnitude. In either case the curves retain their characteristic shapes. As an independent check on our prescription, a neutron wave function has been taken from Hartree calculations.[5] The resulting (p, π^+) calculations do not differ appreciably from those using the above prescription. The study done by Miller[6] using a nonrelativistic DWBA approach shows that for the case of $^{12}C(p,\pi^+)^{13}C_{g.s.}$, a change in the bound state radial parameter also produces angular as well as normalization shifts in the angular distribution. However, it is interesting to note that the sense of the shifts is opposite to that which we observe here. Moreover, the
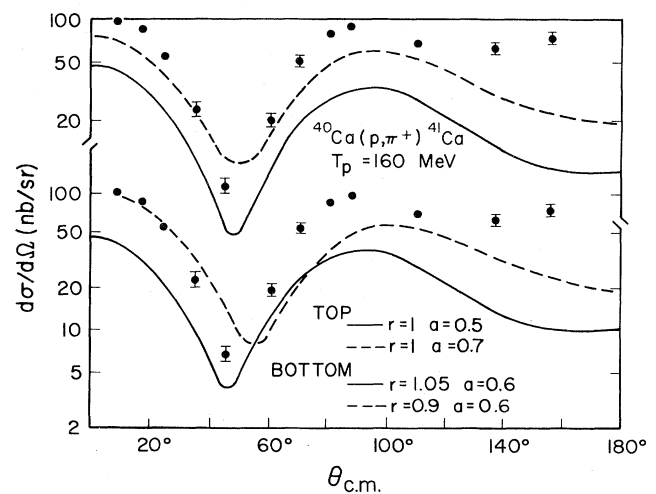

FIG. 1. The effect on the (p, π^+) cross section of altering the geometry parameters of the potentials used in calculating the bound-state wave function. The parameters r and a are the radius and diffuseness parameters of Woods-Saxon potentials. The calculations are carried out for the $^{40}Ca(p,\pi^+)^{41}Ca_{g.s.}$ at $T_p = 160$ MeV. The data are from Ref. 14.

sensitivity we observe here to the radial parameter is much less than that calculated in the nonrelativistic model for the same reaction on ^{12}C by Hoistad et al.[7] We have also studied the effects of variations in the geometry parameters of the bound state potentials on the analyzing power A_y. The results are shown in Fig. 2, for the same value of r and a as in Fig. 1. We find that a change in diffuseness from 0.5 to 0.7 fm produces generally minor changes in A_y, with the most noticeable effect being the enhancement of the positive peak in A_y near 60°. On the other hand, A_y shows more sensitivity to the radial parameter, as is shown in the bottom portion of Fig. 2. An increase in r from 0.9 to 1.05 fm leads to a forward angular shift in A_y of about 10°. There is an upward shift in the analyzing power at forward angles, while A_y becomes slightly more negative at large angles.

We now turn to the more interesting question of the pion distortion. It was shown in Ref. 4 that the distortion of the pion wave function has drastic effects upon both the cross section and analyzing power for the (p,π^+) reaction; it appears almost as if the shapes of the differential cross section and analyzing power are governed by the pion potentials. The question of how sensitive the calculations are to unknowns in these pion-nucleus optical potentials is, therefore, a crucial one which we now address. We have restricted ourselves to considering only pion optical potentials which we feel have a reasonable (albeit nonrelativistic) theoretical basis, and give a good account of both pionic atom data and pion elastic scattering data. We have selected ten potentials[8-10] which we feel satisfy these criteria. These potentials explicitly incorporate many effects such as the angle transformation and the Lorentz-Lorenz-Ericson-Ericson effect. Furthermore, because their parameters are adjusted to get a fit to the pion
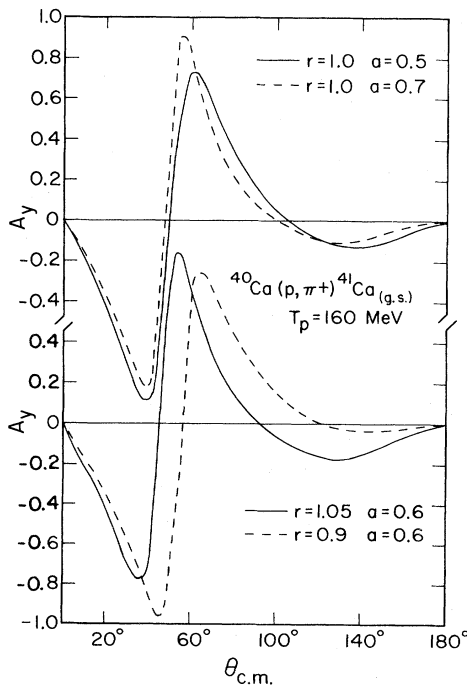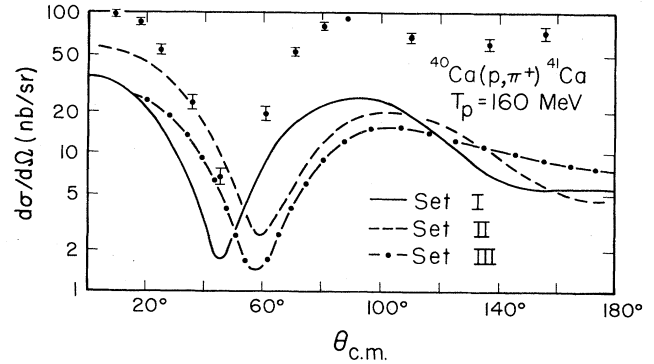

FIG. 3. The effect on the (p,π^+) cross section of using different pion potentials. The curves are produced using pion potential sets I, II, and III described in the text. The calculations are carried out for the reaction ^{40}Ca$(p,\pi^+)^{41}$Ca$_{g.s.}$ at $T_p = 160$ MeV. The data are from Ref. 14.

elastic scattering data, they include many other effects implicitly. In Figs. 3 and 4 we show calculations for three of these potentials. We have chosen these so as to provide an approximate envelope to all ten curves, i.e., the variations between the three curves are typical of those seen with all ten. The three potentials used here are the following: set 1 from Ref. 8 (which is used in Figs. 1, 2, 5, and 6), extrapolated set A from Ref. 9, and set E from Ref. 10. In Figs. 3 and 4, these three sets of pion potentials are referred to as set I, II, and III, respectively. These potentials are discussed at length in the references, but we would like to expound on one desirable feature not emphasized there. Pion potentials based on purely Kisslinger-type terms exhibit a pathological behavior known as a "P-wave catastrophe." This happens because the Kisslinger potentials contain a term which behaves like the kinetic energy operator. When this term is added to the ordinary kinetic energy term the equation behaves like a Schrödinger equation with a position dependent mass. At some value of the radial parameter this effective mass can become infinite and cause kinks in the wave functions.[6] All potentials we have used here are free of

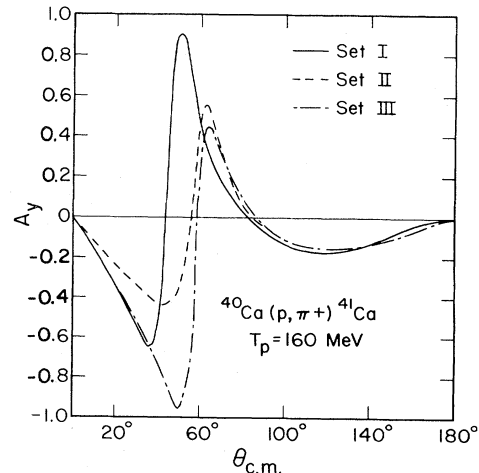FIG. 2. The same as Fig. 1 but for the analyzing power.

FIG. 4. The same as Fig. 3 but for the analyzing power.

this undesirable feature and lead to smooth wave functions.

The elastic scattering predictions from these pion potentials are quite similar in shape, although they may differ in magnitude by around a factor of 2. This can be compared to the spread in (p,π^+) predictions, based on these potentials, as shown in Fig. 3. The main differences between the curves are seen to be a shift in the position, as well as a change in the depth, of the minimum. This amount of sensitivity persists on other nuclei at other energies, the differences between the curves becoming slightly larger with increasing energy. In Fig. 4 we show the dependence of the analyzing power on the pion distortion potentials. Here the peak and minimum of A_y show a considerable smattering of values; however, the characteristic shape of the analyzing power does not vary.

The remaining potentials which are used as input to the calculations are the proton distorting potentials. The effect of taking different proton distorting potentials (subject to the constraint to fitting the elastic scattering data) is shown in Refs. 4 and 11. Just as for the pion distortions, there are small shifts in the normalizations and angles but no qualitative changes, provided that good elastic scattering data exist to constrain the distorting (optical) potentials.

Inherent in the DWBA calculations reported so far is the zero range approximation. This physically restricts the pion to be created at the same point in space at which the proton (in an elastic scattering state) turns into a neutron (in a bound state). To fully take into account this finite range of the NNπ vertex would entail evaluating a six-dimensional integral. However, we can estimate the effect quite easily by means of the following manipulation which is similar in spirit to the local energy approximation. We write the finite range T matrix as

$$T = i\sqrt{2} \int d^3r \, d^3r' \Psi(\vec{r}')\gamma_5\gamma^\mu \Psi(\vec{r}')\partial_\mu f_\lambda(\vec{r},\vec{r}')\phi_\pi(\vec{r}) , \quad (2)$$

where the finite range in the vertex is chosen to be of the form

$$f_\lambda(\vec{r},\vec{r}') = \frac{\lambda^2 e^{-\lambda|\vec{r}-\vec{r}'|}}{4\pi|\vec{r}-\vec{r}'|} = \sum_{n=0}^{\infty} \frac{[\nabla^2]^n}{[\lambda^2]^n}\delta(\vec{r}-\vec{r}') . \quad (3)$$
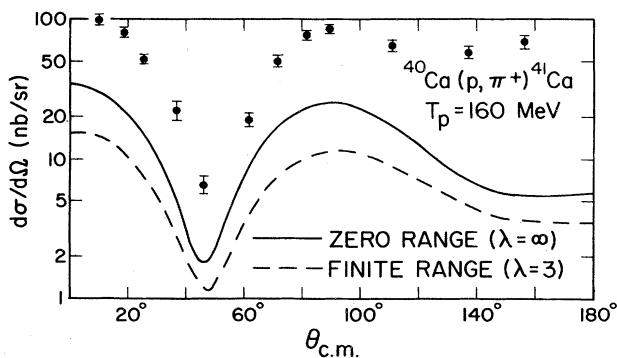
From fitting pion nucleon elastic scattering data,[12,13] the parameter λ is estimated to be 3 fm^{-1}. To obtain the expression for the finite range, we truncate the series in (3) to two terms and substitute them into Eq. (2). Green's theorem may now be used to turn the ∇^2 onto the pion wave function, where it can be replaced by the pion potential by using the Klein-Gordon equation satisfied by the pion wave function. Finally this process may be Padé accelerated[15] (it turns out that the Padé acceleration has little effect).

Figure 5 illustrates the finite range effects on the calculated cross sections. We compare the ZR result ($\lambda = \infty$) shown by the dashed curve to the finite range (FR) one for the case $\lambda = 3$ (solid curve). It is seen that the main effect of taking the finite range into account is to cause a downward shift in the calculated cross section. On the other hand, we find very little effect on the calculated analyzing powers. This is shown in Fig. 6.

In summary, we have investigated some of the sensitivities of the cross section and analyzing power for the (p,π^+) reaction, in the framework of the relativistic one nucleon DWBA model, to ambiguities in the input parameters as well as to finite range effects. We find that the latter has little effect on the calculated analyzing power, but leads to a decrease in the magnitude of the cross section [$\sim 50\%$ for ^{40}Ca$(p,\pi^+)^{41}$Ca$_{g.s.}$ at 160 MeV]. Both observables also show some sensitivity to the bound state geometry. We find that variations in the geometry can produce normalization as well as angle shifts in the observables, but none can be regarded as drastic (with, say, 30% change in diffuseness or 15% change in the radial parameter). We have looked at the impact of the ambiguity in the pion optical potentials on the calculated (p,π^+) observables. Comparison of three different realistic potentials (which are free of the P-wave catastrophe) show that in general one is left with uncertainties in cross section normalization in addition to angular shifts in both

FIG. 5. Zero-range ($\lambda = \infty$) and finite-range ($\lambda = 3$) calculations for the ^{40}Ca$(p,\pi^+)^{41}$Ca$_{g.s.}$ cross section at $T_p = 160$ MeV. The finite range calculations are carried out using the approximation described in the text. The data are from Ref. 14.
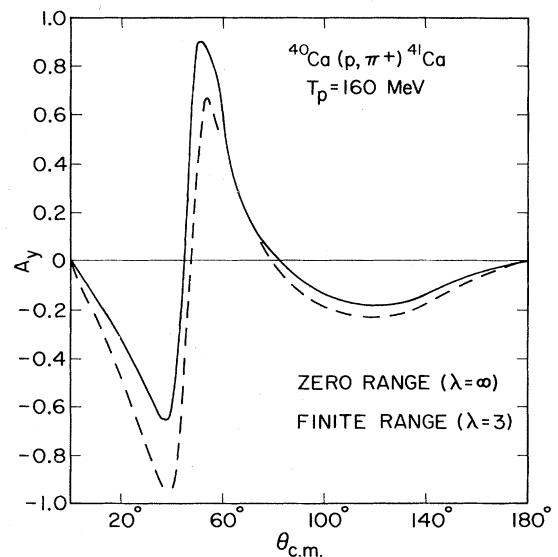

FIG. 6. The same as Fig. 5 but for the analyzing power.

cross section and analyzing power as a result of the ambiguities in the pion potentials. However, the overall shapes are reasonably free from ambiguity.

---

[1]L. D. Miller and H. J. Weber, Phys. Lett. **64B**, 279 (1976).

[2]R. Brockmann and M. Dillig, Phys. Rev. C **15**, 361 (1977).

[3]E. D. Cooper and H. S. Sherif, Phys. Rev. Lett. **47**, 818 (1981).

[4]E. D. Cooper and H. S. Sherif, Phys. Rev. C **25**, 3024 (1982).

[5]C. Horowitz, private communication.

[6]C. A. Miller, Nucl. Phys. **A224**, 269 (1974).

[7]B. Hoistad, S. Dahlgren, , P. Grafstrom, and A. Asberg, Phys. Scr. **9**, 201 (1974).

[8]K. Stricker, H. McManus, and J. A. Carr, Phys. Rev. C **19**, 929 (1979).

[9]K. Stricker, J. A. Carr, and H. McManus, Phys. Rev. C **22**, 2043 (1980).

[10]J. A. Carr, H. McManus, and K. Stricker-Bauer, Phys. Rev. C **25**, 952 (1982).

[11]E. D. Cooper, Ph. D. thesis, University of Alberta, 1981 (unpublished).

[12]I. Afnan and B. Blankleider, Phys. Rev. C **24**, 1572 (1981).

[13]B. Blankleider, private communication.

[14]P. H. Pile, R. D. Bent, R. E. Pollock, P. T. Debevec, R. E. Marrs, M. C. Green, T. P. Sjoreen, and F. Soja, Phys. Rev. Lett. **42**, 1461 (1979).

[15]G. Baker, *Padé Approximates in Theoretical Physics* (Academic, New York, 1970).